FFI RAPPORT

MODELLING OF ELECTROMAGNETIC INFLUENCES FROM WIND FARMS AT FREQUENCIES BELOW 30 MHZ – Interference and scattering

OTNES Roald

FFI/RAPPORT-2007/00086

MODELLING OF ELECTROMAGNETIC INFLUENCES FROM WIND FARMS AT FREQUENCIES BELOW 30 MHZ – Interference and scattering

OTNES Roald

FFI/RAPPORT-2007/00086

FORSVARETS FORSKNINGSINSTITUTT
Norwegian Defence Research Establishment
P O Box 25, NO-2027 Kjeller, Norway

FORSVARETS FORSKNINGSINSTITUTT(FFI)
Norwegian Defence Research Establishment

P O BOX 25
NO-2027 KJELLER, NORWAY

UNCLASSIFIED

SECURITY CLASSIFICATION OF THIS PAGE
(when data entered)

REPORT DOCUMENTATION PAGE

1) PUBL/REPORT NUMBER	2) SECURITY CLASSIFICATION	3) NUMBER OF PAGES
FFI/RAPPORT-2007/00086	UNCLASSIFIED	37
1a) PROJECT REFERENCE	**2a) DECLASSIFICATION/DOWNGRADING SCHEDULE**	
FFI-II/1013/912	-	

4) TITLE

MODELLING OF ELECTROMAGNETIC INFLUENCES FROM WIND FARMS AT FREQUENCIES BELOW 30 MHZ – Interference and scattering

5) NAMES OF AUTHOR(S) IN FULL (surname first)

OTNES Roald

6) DISTRIBUTION STATEMENT

Approved for public release. Distribution unlimited. (Offentlig tilgjengelig)

7) INDEXING TERMS

IN ENGLISH	IN NORWEGIAN
a) Wind turbine	a) Vindmølle
b) Wind farm	b) Vindkraftverk
c) High frequency radio	c) HF-radio
d) Electromagnetic interference	d) Elektromagnetisk interferens
e) Scattering	e) Spredning

THESAURUS REFERENCE:

8) ABSTRACT

This report describes models for electromagnetic influences from wind farms at frequencies below 30 MHz. Regarding radiated electromagnetic interference, a methodology based on well-established models is proposed.

Regarding scattering and direction finding error, a model inspired by previous reports and measurements is proposed. Due to large remaining uncertainty in important input parameters, the scattering model can presently only provide order-of-magnitude estimates.

The models developed in this work can be used to evaluate concerns on whether planned wind farm installations can have negative impact on military systems utilizing frequencies below 30 MHz.

9) DATE	AUTHORIZED BY	POSITION
2007-01-11	This page only Vidar S Andersen	Director

ISBN 978-82-464-1073-9

FFI-B-22-1982

UNCLASSIFIED

SECURITY CLASSIFICATION OF THIS PAGE
(when data entered)

CONTENTS

page

MODELLING OF ELECTROMAGNETIC INFLUENCES FROM WIND FARMS AT FREQUENCIES BELOW 30 MHZ

Interference and scattering

1 INTRODUCTION

This report summarizes work on modelling of electromagnetic influences (radiation and scattering) from wind farms at frequencies below 30 MHz. The models developed can be used to evaluate concerns on whether planned wind farm installations can have negative impact on military systems utilizing such frequencies, in particular sensitive receiver and direction finding stations.

The work presented here has been performed under project 1013 “Effekt av vindkraftutbygging på radiosamband og radar (VINDKRAFT)” (The effect of wind power development on telecommunications and radar) at the Norwegian Defence Research Establishment (FFI). It is a follow-up to the previous report [14], where a measurement campaign at Smøla suggested that the scattering effects at 2 and 10 MHz from a wind farm may be significantly larger than previously expected. The scattering model developed is partly based on previous work by FOI in Sweden and partly by experiences from the measurement campaign at Smøla. There are however large uncertainties involved in input parameters to the model, due to the limited extent of the measurement data from Smøla.

The work on electromagnetic interference (EMI) due to possible radiation from wind turbines is motivated by the fact that as far as we have been able to establish, there exist no applicable regulations regarding electromagnetic radiation from wind turbines. A model is presented which extrapolates candidate field strength limits from a measurement distance near a wind turbine to the receiver position farther away. Standard EMC (electromagnetic compatibility) regulations include provision for setting specific radiation limits in the vicinity of sensitive receiver sites, and the proposed model can be used as a tool when agreeing on such limits.

Sec. 2 discusses ground wave propagation, an important factor in both models. Sec. 3 discusses electromagnetic interference due to radiation, including an overview of existing standards and regulations, and presents the proposed model. Sec. 4 presents the proposed model for scattering, compares it to a previous model by FOI and discusses all the uncertainties presently associated with the proposed model. For both proposed models (interference in Sec. 3 and scattering in Sec. 4), recommendations on usage and input parameters are presented as well as examples using the geometry from the measurement campaign at Smøla. Finally, conclusions are given in Sec. 5.

The final software delivery from project 1013 will be the WTES (Wind Turbines & Electromagnetic Systems) software. The models and algorithms described in this report are currently implemented in Matlab, and are intended to be the groundwork for the HF module in WTES.

The work presented in this report has mostly been performed in the time frame

October-December 2006.

2 GROUND WAVE PROPAGATION

One issue common to the problems of EMI due to radiation and scattering from wind farms, is the estimation of path loss of HF radio waves from the wind farm to the receiver site. The dominant mode of propagation for distances of interest (up to approximately 50 km) is ground wave, where the energy propagates partly along the ground/air-interface and partly in air.

2.1 Background

The ground wave path loss should be estimated using the GRWAVE software program, developed and recommended by ITU-R in Rec. P.368-7 [13]. The program is stated to be valid in the frequency range 10 kHz - 30 MHz. The input parameters of interest are ground conductivity and permittivity, as well as polarization and transmitter and receiver height above ground. Maps of ground conductivity in different countries (mostly determined by measuring path loss at a frequency of 1 MHz) are found in ITU-R Rec. P.832-2 [3]. The map for Norway is reproduced in Fig. 2.1. Note that these values are quantized at two levels per decade, and do not incorporate seasonal and weather-induced variations. Ground conductivity depends on the moisture content of the ground and is hence increased during wet seasons, but snow cover will not influence the conductivity significantly, as snow mostly consists of non-conductive fresh water.

In ITU-R Rec. P.527-3 [1] are given standardized conductivity and permittivity values for different types of ground, as function of frequency. They are mostly independent of frequency in the range 100 kHz – 10 MHz, with values as summarized in Table 2.1.

Ground type	Conductivity σ_g	Relative permittivity ϵ_r
Sea water (average salinity)	5 S/m	70
Fresh water, 20° C	3 mS/m	80
Pure water, 20° C	0-2 mS/m	80
Ice (fresh water)	15-80 μS/m	3
Wet ground	10 mS/m	30
Medium dry ground	1 mS/m	15
Very dry ground	0.1 mS/m	3

Table 2.1 Standardized ground conductivity and permittivity values in the frequency range 0.1-10 MHz for different ground types, from [1, Figure 1].

It will simplify the analysis to relate the transmission path loss of ground wave propagation to the free space path loss L_{fs}, given by the following equation:

$$L_{fs}(f,d) = \left(\frac{4\pi d}{\lambda}\right)^2 \tag{2.1}$$

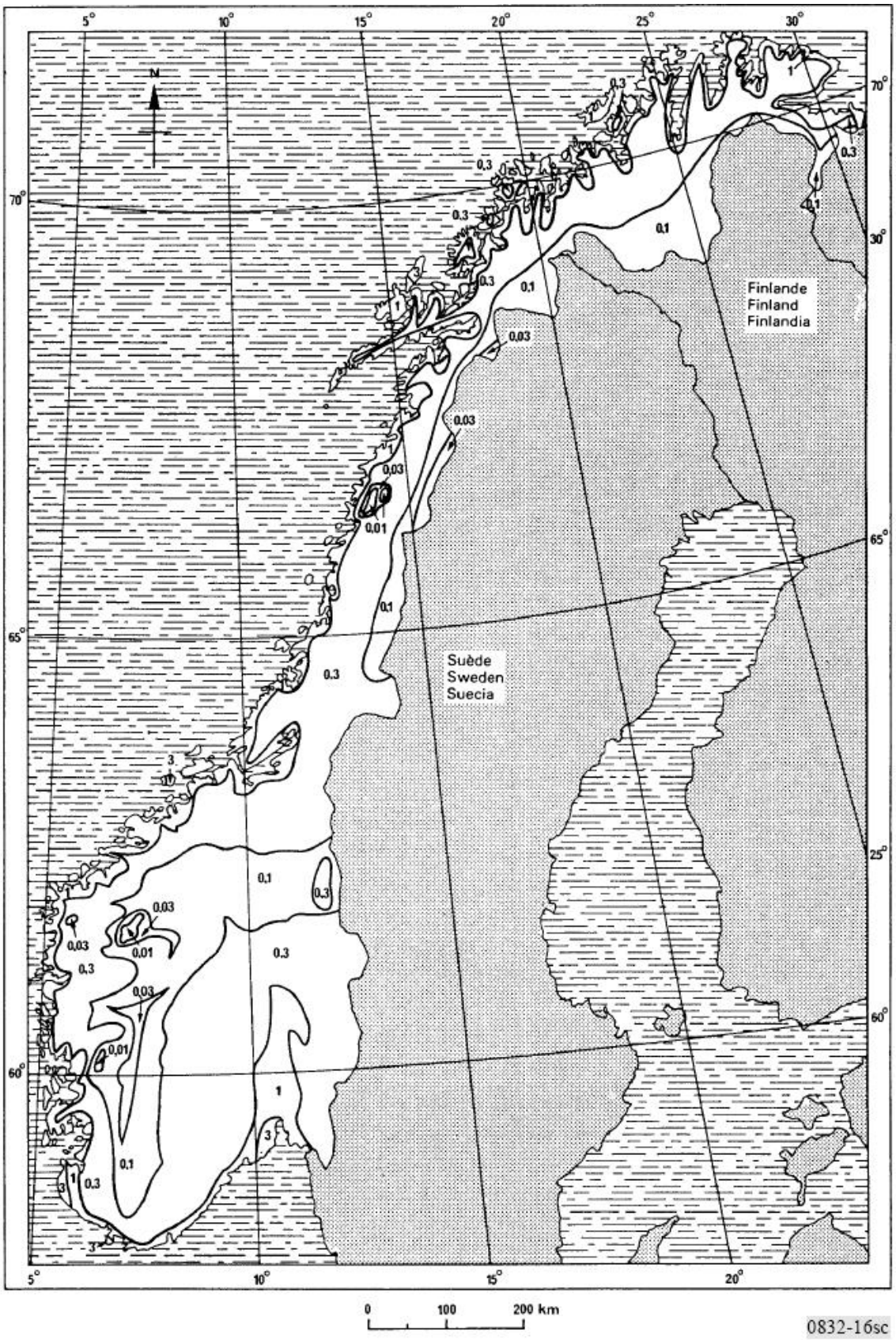

Figure 2.1 Ground conductivity map of Norway, from [3]. Numbers are given in units of mS/m.

where d is distance from transmitter and $\lambda = c/f$ is the wavelength. In dB units this corresponds to

$$L_{fs}[\text{dB}] = -147.6 + 20\log_{10}(d[\text{m}]) + 20\log_{10}(f[\text{Hz}]) \tag{2.2}$$

i.e., a 20 dB/decade roll-off with distance, resulting directly from spherical spreading.

The ground wave path loss L_g can be decomposed into the free space path loss and an excess loss L_{ex} due to absorption in the ground, as follows:

$$L_g[\text{dB}] = L_{fs}[\text{dB}] + L_{ex}[\text{dB}] \tag{2.3}$$

L_{ex} will in general be positive, but may be slightly negative for propagation over sea water. It is lower bounded by –3 dB, which is the value for the case of an elevated antenna over a flat perfectly conducting ground, with the energy spreading losslessly on the half-sphere above ground.

In the case of ground parameters varying along the propagation path (e.g., crossing a fiord), the overall path loss can be estimated using a method called “Millington’s method”, as an extension to GRWAVE (see e.g. Annex 2 of [13]). FFI has a Matlab implementation of Millington’s method [12] which is included in the software delivery from the project.

In the case of distinct topographic features between transmitter and receiver, like a big mountain or deep valley, the GRWAVE result will be inaccurate. The exact prediction of path loss under such circumstances is not a mature field [12], but in general a mountain will increase the path loss while a valley will lead to lower path loss (closer to free space). The recommendation in [13, Note 5] is to compute the average terrain elevation along the path, and if the terrain elevation at the transmitter/receiver is *above* this value, the effective antenna height is found by adding the difference to the actual antenna height above ground. If the terrain elevation at the transmitter/receiver is *below* the average terrain elevation, the effective antenna height is set equal to the actual antenna height above ground.

2.2 Recommendations

We recommend the following approach for selecting ground parameters for modelling of ground wave path loss:

- Select σ_g as the maximum ground conductivity in the region of interest, from the map in Fig. 2.1.
- Select ϵ_r based on σ_g such that one of the following parameter combinations is used:
  $\sigma_g \leq 0.1$ mS/m, $\quad \epsilon_r = 3$
  $\sigma_g = 0.3$ mS/m, $\quad \epsilon_r = 7$
  $\sigma_g = 1$ mS/m, $\quad \epsilon_r = 15$
  $\sigma_g = 3$ mS/m, $\quad \epsilon_r = 22$
  $\sigma_g = 10$ mS/m, $\quad \epsilon_r = 30$
  $\sigma_g = 30$ mS/m, $\quad \epsilon_r = 40$
  These values are based on Table 2.1, and on parameter combinations used for curves presented in [13].

- The ground parameters obtained in this manner are best estimates from readily available sources. If more detailed knowledge of ground parameters in the vicinity of the receiver site is available, this should be taken into account.

At low frequencies, it may occur that the transmission distance d becomes comparable to the wave length λ. If the minimum distance input to the GRWAVE software from ITU-R is below 2λ, GRWAVE automatically changes the minimum distance to 2λ, even though the curves in [13] do not suffer from this restriction and a modification equation for the near field is given in [13, Note 3]. Hence, the practical lower frequency limit for application of GRWAVE is

$$f_{\text{min,GRWAVE}} = \frac{2c}{d} \tag{2.4}$$

where c is the speed of light.

We recommend setting the basic transmitter height equal to the height of the wind turbine tower for EMI calculations, and equal to zero for scattering calculations.

We recommend setting the basic receiver height equal to zero for ground-mounted vertical receiver antennas, and equal to the antenna height for elevated beam antennas.

If the wind turbine/receiver location is higher than the average terrain elevation along the path (e.g., if crossing a valley), we recommend using an effective antenna height which is the basic antenna height as defined above, plus the height of the wind turbine/receiver location above the average terrain elevation along the path [13, Note 5].

We recommend setting the ground wave polarization to vertical for all cases, as the path loss for horizontally polarized wave will be very large and not contribute to any influences from the wind farm.

When the radio path crosses partly land and partly sea, we recommend using the Millington extension to GRWAVE to estimate the overall path loss. Millington's method gets complicated when there is a large number of sea/land transitions, and we therefore recommend simplifying the actual geometry to a few (one or two) sea/land transitions, rather than using all the actual transitions along the path.

2.3 Sensitivity to parameters

The most important parameters are ground conductivity and permittivity. Fig. 2.2 shows the ground wave transmission loss as function of distance for different parameter combinations, for a transmitter height of 70 m.

Note that over sea water the ground wave path loss is close to the free space equation (2.2), while over land there is an excess loss of tens of dB. The excess loss increases with increasing frequency and with increasing distance. The variation among the different (non-sea) ground types shown is approximately 20 dB at 500 kHz and 2 MHz, and approximately 6 dB at 10 MHz. Investigating the effect of conductivity and permittivity separately (not shown here), it is found that conductivity is the most important of the parameters at 500 kHz, while the variation at 10 MHz is due to the different permittivities. At 2 MHz, both parameters contribute to the variation. See also [12].

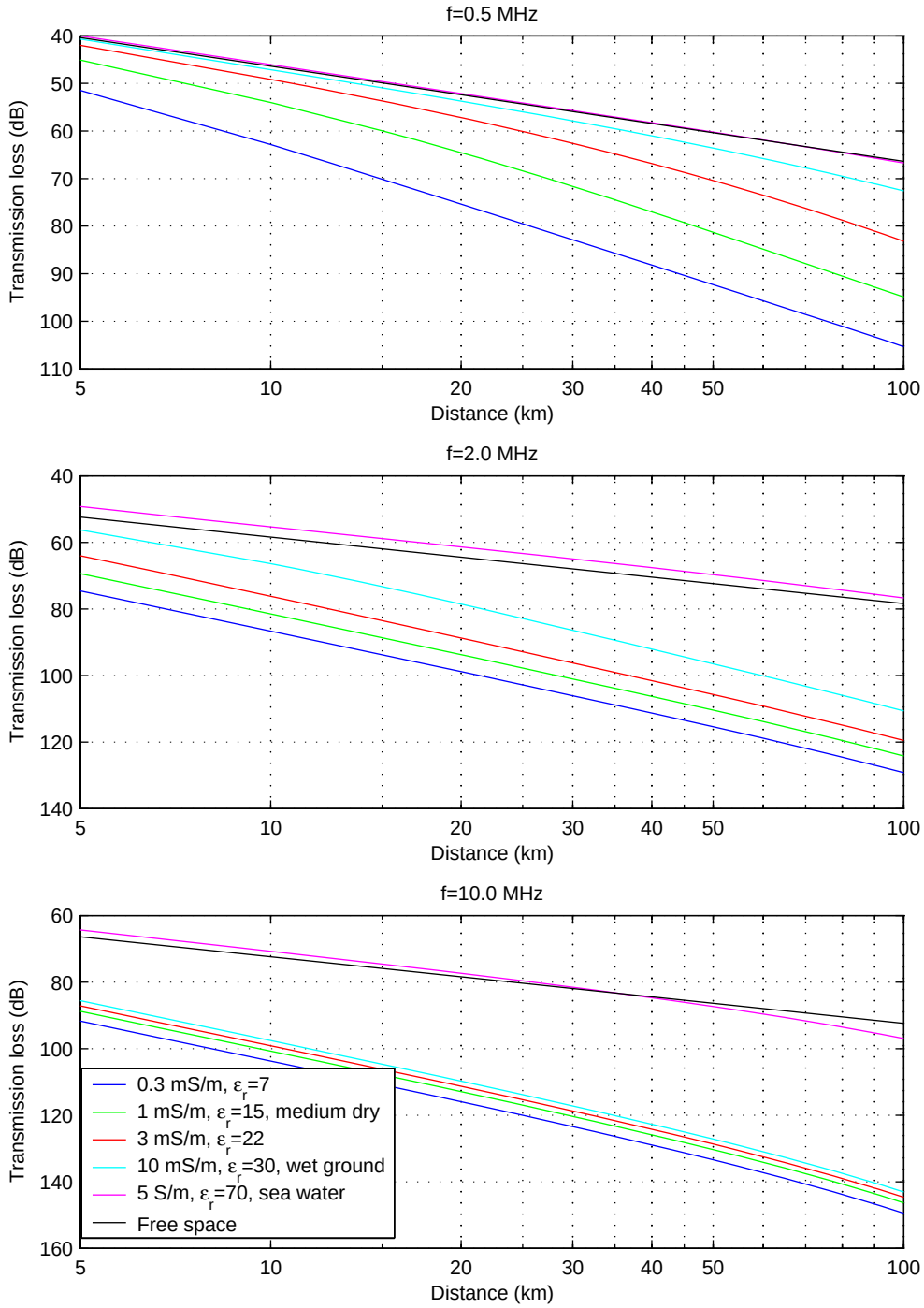

*Figure 2.2 Ground wave transmission loss as function of distance for different ground parameters and frequencies. Transmitter height is **70 m**, receiver height is 0 m, and vertical polarization is applied.*

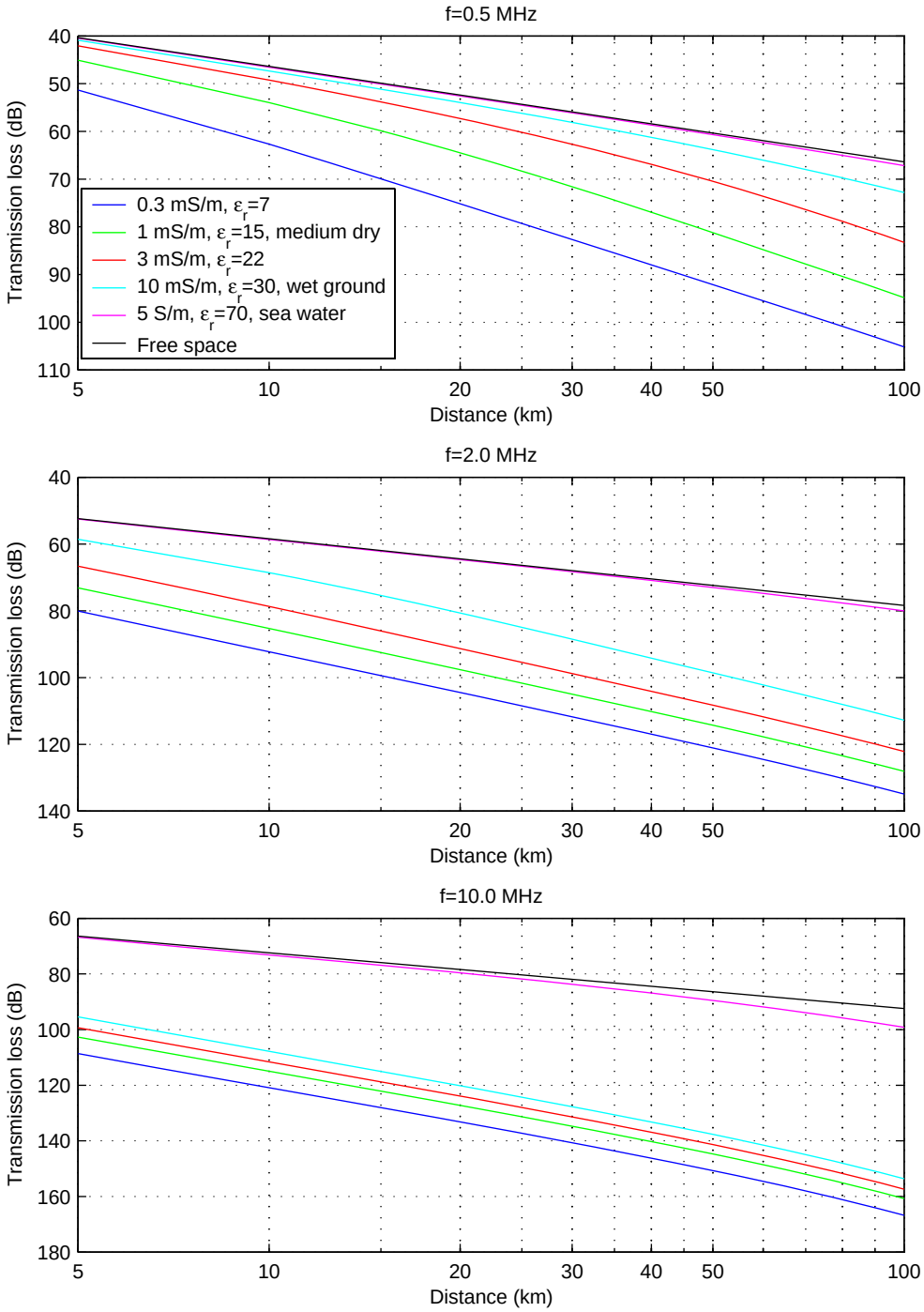

*Figure 2.3 Ground wave transmission loss as function of distance for different ground parameters and frequencies. Transmitter height is **0 m**, receiver height is 0 m, and vertical polarization is applied.*

In Fig. 2.3 the transmitter height has been reduced from 70 m to 0 m. We find that the difference between a transmitter height of 70 m and 0 m is negligible at 500 kHz, approximately 6 dB at 2 MHz, and more than 30 dB at 10 MHz (the path loss is higher with a transmitter height of 0 m compared to 70 m).

3 ELECTROMAGNETIC INTERFERENCE DUE TO RADIATION FROM WIND FARMS

3.1 Background

The major civilian standard regarding EMC measurement apparatus and methods is CISPR 16 (equivalent to EN55016), which consists of several parts. Regulations on EMC properties of different types of (non-military) equipment typically defines certain limits, and refers to CISPR 16 regarding how the measurements should be performed. The parts of CISPR 16 relevant to radiation in the HF frequency range are as follows:

CISPR 16-1-1 [8] describes requirements to hardware used for EMC measurements, e.g. the often-used “quasi-peak” and “peak” detectors, and specifies the measurement bandwidth in the frequency range 0.15-30 MHz to be 9 kHz. CISPR 16-1-4 [9] describes requirements to measurement antennas, and CISPR 16-2-3 [10] describes measurement methods. CISPR 16-4-4 [5] discusses how to relate limits to protection requirements.

Limits on unintentional radiated electromagnetic interference (EMI) from equipment is in general given as field strength at a certain “measurement distance” away from the equipment, in a certain measurement bandwidth. The limit may be given as electric field strength (dBμV/m) or magnetic field strength (dBμA/m). The ratio between the two *in the far field* is given by the free space impedance of $Z_0 = 377\Omega$, or in dB units

$$E[\text{dB}\mu\text{V/m}] = H[\text{dB}\mu\text{A/m}] + 51.5 \tag{3.1}$$

It should be noted that this equation is often used in practice also in the near field, when a loop antenna is used to measure the magnetic field strength, but the result is given in electrical field strength units (dBμV/m). As the ratio between magnetic and electric field strength is not constant in the near field, this conversion introduces an error of unknown magnitude when used at measurement distances shorter than one wavelength.

Regarding EMC limits applicable to wind farms, we have not been able to find any relevant limits on electromagnetic radiation at frequencies below 30 MHz. Wind turbines is a type of equipment that should be covered by CISPR 11 [7], but this standard only defines relevant conducted (not radiated) emission limits for frequencies below 30 MHz. CISPR 11 does however include provision for national authorities to specify additional rules in the vicinity of specific sensitive radio sites, in subclause 5.4.

We have identified two standards, designed for other types of equipment, defining limits on electromagnetic radiation at HF frequencies and below. These are Section 5.16 of MIL-STD-461E [2], the EMC standard for military equipment, and NB30 [4] (NB = Nutzungsbestimmung = usage provision), the German regulation for power line

telecommunications (PLT) systems. Ref. [2, Section 5.16] specifies different limits for different types of platforms, in the range 24-44 dBμV/m at HF frequencies (referred to a measurement distance of 1 m and measurement bandwidth of 10 kHz). Ref. [4] specifies the following limits, referred to a measurement distance of 3 m:

$$E_{\text{NB30}}[\text{dB}\mu\text{V/m}] = 40 - 20\log_{10}(f[\text{MHz}]), \text{ in the frequency range 9 kHz - 1 MHz} \quad (3.2)$$

$$E_{\text{NB30}}[\text{dB}\mu\text{V/m}] = 40 - 8.8\log_{10}(f[\text{MHz}]), \text{ in the frequency range 1-30 MHz} \quad (3.3)$$

The measurement bandwidth specified in NB30 is 9 kHz in the frequency range 0.15-30 MHz, and 200 Hz in the frequency range 9-150 kHz.

In case of free space propagation, the relationship between field strengths at two different distances in the far field can be deduced from Eqn. (2.2), where the constant and frequency-dependent terms cancel out:

$$E(d)[\text{dB}\mu\text{V/m}] = E(d_0)[\text{dB}\mu\text{V/m}] - 20\log_{10}(d/d_0) \quad (3.4)$$

Here, $E(d_0)$ can be taken as the allowed radiation limit, and d_0 as the associated measurement distance. In the near field to the radiating equipment, the roll-off with distance is generally steeper than the 20 dB/decade implied by Eqn. (3.4) [5, subclause 5.3.1]. Hence, if the measurement distance d_0 is in the near field, applying this equation will over-estimate the field strength in the far field.

Ideally, the measurement distance should be large enough to be in the far field for all measured frequencies, as this will make the above-mentioned approximations exact (conversion from magnetic to electric field strength, and 20 dB/decade distance conversion). However, at too large measurement distances the limit may be lower than other ambient noise sources, and it will not be possible to measure compliance. There is therefore always a trade-off involved in the selection of measurement distance. Note that if the equations are applied at measurement distances in the near field where they are not strictly valid, applying Eqn. (3.4) will always over-estimate the field strength in the far field, while it is unknown whether Eqn. (3.1) will under- or over-estimate the electrical field strength.

3.2 Recommendations

3.2.1 Limits

As no relevant standards for electromagnetic radiation from wind farms have been established to our knowledge, we recommend that specific limits are agreed upon in each case, depending on the distance between wind farm and receiver site and the total number of wind turbines installed.

A wind turbine is too large for EMC measurement chambers, hence *in situ* measurements are required. Measurements should be performed on a single wind turbine, with the remaining turbines in the wind farm turned off.

When specific limits are established, we recommend the measurement distance d_0 to be approximately equal to the nacelle height above ground, as a trade-off between achieving

far-field conditions and ensuring that the limit value is above the ambient noise level. We recommend the measurement height above ground to be as high as possible (in order to minimize the influence of local ground conditions), preferably it should be in the same horizontal plane as the nacelle. The practical implication of this is that either a long non-conductive mast or a helicopter is required in order to make the measurement.

To establish limit values for the electrical field strength in a particular case, we recommend using numbers from MIL-STD-461E or NB30 directly as a starting point (without adjustment for measurement distance). Then, the resulting field strength at the receiver site should be predicted with the method described below, and the limit values adjusted according to the result. Measurability should also be taken into account, as setting the limit too low will cause many frequencies to be unmeasurable due to other ambient "noise" sources (e.g., broadcasting stations).

We recommend specifying limits with peak measurements rather than quasi-peak, as this will allow for a quicker measurement procedure, and is also easier to interpret.

3.2.2 Background noise levels

The actual sensitivity of a sensitive receiver site will often be classified information. For easier handling, we therefore recommend to rather compare the estimated interference level at a sensitive receiver site to established noise curves, e.g., as found in ITU-R Rec. P.372-8 [6]. As sensitive receiver sites are generally located in low-noise regions, we recommend comparison to the "quiet rural" noise curve, converted to electrical field strength by combining equations (11) and (7) of [6]:

$$\begin{aligned} E_{qr}(f)[\text{dB}\mu\text{V/m}] &= 53.6 + (20 - 28.6)\log_{10}(f[\text{MHz}]) + 10\log_{10}(b[\text{Hz}]) - 95.5 \\ &= -41.9 - 8.6\log_{10}(f[\text{MHz}]) + 10\log_{10}(b[\text{Hz}]) \end{aligned} \tag{3.5}$$

where b is the measurement bandwidth (usually 9 kHz, corresponding to 39.5 dBHz). See also Fig. 3.1 later in the report.

The ITU-R curve for man-made noise in quiet rural areas, Eqn. (3.5), dominates over natural noise sources in the frequency range 70 kHz-5 MHz. Above 5 MHz, galactic noise dominates but is only a few dB above Eqn. (3.5). Below 70 kHz, atmospheric noise dominates significantly. Thus, the recommended frequency range for application of Eqn. (3.5) is 70 kHz-30 MHz.

As a more stringent alternative, one could apply the "Absolute Protection Requirement" proposed by the NATO RTO Task Group "IST-050/RTG-022 on HF Interference, Procedures, and Tools"[1]. The Absolute Protection Requirement is based on *minimum* measured noise levels at quiet receiver sites, and is –15 dBμV/m (in 9 kHz bandwidth) at the receiver site, flat across the frequency range 1.5-30 MHz. This is slightly below the ITU-R quiet rural curve, which is based on *median* noise levels.

[1] This task group has considered EMC problems related to power line telecommunications (PLT), and the author of the present report has been Norway's representative to the task group. The final report of the task group will be published early 2007.

Yet another alternative is to use historical data from the sensitive receiver station to estimate the noise floor at that particular site. This may, however, be classified data and hard to make use of in practice.

3.2.3 Estimating EMI from a single wind turbine

We recommend estimating the electromagnetic interference level at a sensitive receiver site, from a single wind turbine, using the following equation:

$$E_1(f,d)[\text{dB}\mu\text{V/m}] = E(d_0)[\text{dB}\mu\text{V/m}] - 20\log_{10}(d/d_0) - L_{ex}(f,d)[\text{dB}] \tag{3.6}$$

where

- $E(d_0)$ is the allowed radiation limit, and d_0 is the associated measurement distance (from the radiating equipment).
- d is the distance between radiating equipment and receiver site
- $E_1(f,d)$ is the interference field strength at the receiver site at frequency f, at a distance d from the radiating equipment. The field strength is referred to the same measurement bandwidth as used in the limit definition (in general 9 kHz in the HF band). The subscript "1" denotes that this is the contribution from a single wind turbine.
- $L_{ex}(f,d)$ is the excess path loss of ground wave propagation relative to the free space equation, see Eqn. (2.3).

3.2.4 Estimating cumulative EMI from a wind farm

When a wind farm with a number of wind turbines is installed in the vicinity of a sensitive receiver site, one should take into consideration that the radiated EMI from all the turbines might add up in a cumulative fashion. One could envision three different scenarios in this regard, rated from least to most severe:

1. The radiated EMI from all wind turbines are at different frequencies. No cumulative effect will occur, and the quantity of interest is $E_1(f, d_{\text{min}})$, where d_{min} is the distance to the wind turbine closest to the receiver site.
2. All wind turbines cause radiated EMI at the same frequency(ies), but not coherently. A cumulative effect will occur, where the contribution from all wind turbines are added on a power basis.
3. All wind turbines cause radiated EMI at the same frequency(ies), and coherently (in phase). A cumulative effect will occur, where the contribution from all wind turbines are added on an amplitude basis. This is significantly more severe than adding on a power basis.

We recommend assuming the second scenario, i.e., adding the contributions on a power basis. This recommendation is based on the fact that wind turbines of identical design are likely to radiate at the same frequency(ies), but coherent EMI is unlikely as there is no phase synchronization between the turbines at frequencies above the line frequency (50 Hz) and its first few harmonics.

The cumulative EMI from a wind farm with N wind turbines, when adding the contributions on a power basis, is given by

$$E_N(f)[\text{dB}\mu\text{V/m}] = 10\log_{10}\sum_{i=1}^{N} 10^{\frac{E_1(f,d_i)[\text{dB}\mu\text{V/m}]}{10}} \tag{3.7}$$

where d_i is the distance to the ith wind turbine from the receiver site. Since we have standardized on dB units in this report, we convert to power before summing and back to dB in the end.

For first-order assessments of EMI potential, we recommend assuming all the wind turbines to be at the same distance d to the receiver. Choosing d equal to the minimum distance between wind farm and receiver will give an upper bound on the cumulative EMI. In this case, Eqn. (3.7) simplifies to

$$E_N(f,d)[\text{dB}\mu\text{V/m}] = E_1(f,d)[\text{dB}\mu\text{V/m}] + 10\log_{10} N \tag{3.8}$$

3.2.5 Antenna gain

In case of directive receiver antennas, the maximum achievable antenna gain in the direction of the wind farm should be added to the estimated EMI level at the receiver. The antenna gain should *not* be added to the noise curve, as the background noise can be assumed to arrive isotropically from all directions.

3.2.6 Overall EMI estimation method

To summarize, we recommend the following method to estimate EMI from a wind farm to a sensitive receiver site:

- The starting point is an assumed limit for electrical field strength E at a certain measurement distance d_0 from each wind turbine (alternatively, the method can be applied “backwards” in order to estimate what limits are required if the noise floor at the receiver site should not increase).
- The excess path loss L_{ex} in Eqn. (3.6) is estimated using GRWAVE.
- The EMI at the receiver site caused by a single wind turbine is estimated using Eqn. (3.6).
- The cumulative effect from N wind turbines in a wind farm is estimated using Eqn. (3.8) for first-order assessment, or using Eqn. (3.7) for more detailed evaluation.

- The maximum achievable receiver antenna gain in the direction of the wind farm is added.
- The resulting field strength is compared to the ITU-R quiet rural noise curve of Eqn. (3.5).

3.3 Implementation

The method described above has been implemented as a Matlab function *windfarm_HF_EMI.m*, which takes the following input parameters:

- Geographical coordinates of wind farm and receiver
- Limit value on radiated emission: Electric field strength at multiple frequencies, measurement bandwidth, and measurement distance
- Nacelle height above terrain
- Ground conductivity (permittivity is derived from conductivity as described in Sec. 2.2)
- Receiver antenna gain
- Flag specifying whether plots should be produced or not

The output of the function is the resulting electrical field strength at the receiver site, assuming all wind turbines are radiating at the limit level. The results are given from the simple equation (3.8) as well as from the more exact equation (3.7). The ITU-R quiet rural man-made noise level at the studied frequencies is also output.

The function uses digital elevation data on the DTED format to evaluate the terrain profile along the path between wind farm centroid and receiver, from which the average elevation of the path is computed. Then, the transmitter and receiver heights are set according to the recommendations in Sec. 2.2, assuming all turbines are at the same terrain elevation as the highest wind turbine.

As a minor simplification, the excess loss L_{ex} in Eqns. (2.3) and (3.6) is only evaluated for the distance d_{min} from the receiver to the nearest wind turbine, and this value is used for all wind turbines (while the free space loss component L_{fs} is computed individually for each turbine).

The method is considered for possible future integration into WTES.

3.4 Example

As an example, we use the geometry (wind farm and receiver position) from the Smøla measurement campaign [14], see also Fig. 4.4 later in the present report. We assume the radiation limit from the wind farm is set equal to the NB30 numerical values, but at a measurement distance of 70 m (without decreasing the limit to compensate for the increased measurement distance). The limit assumed in the example is shown in Fig. 3.1.

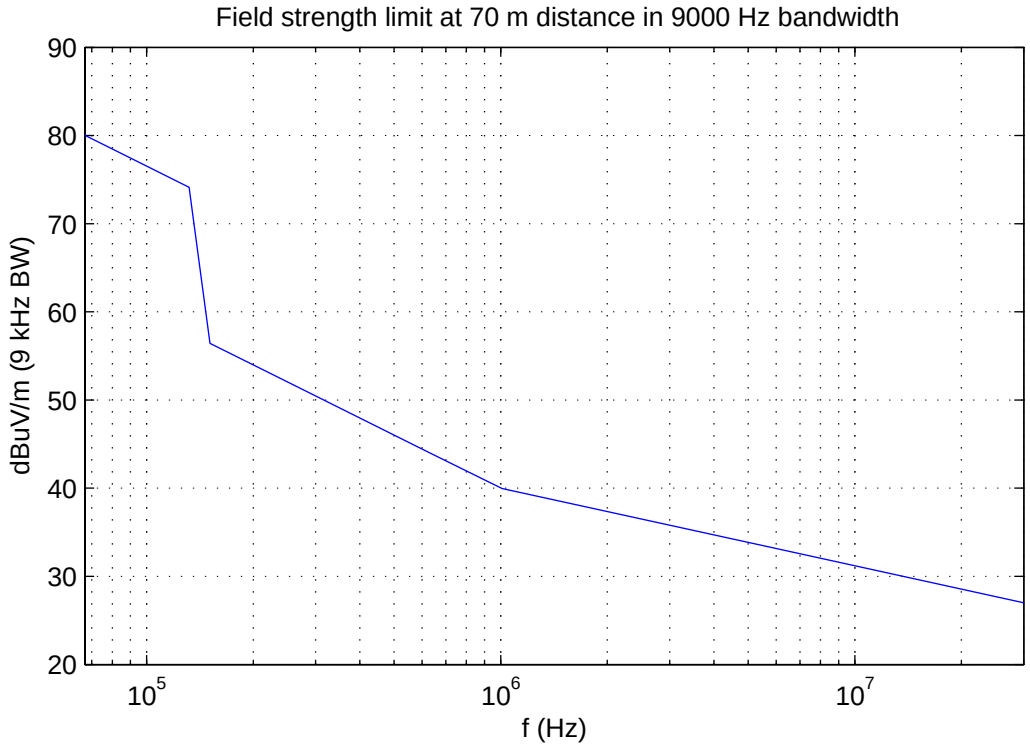

Figure 3.1 Limit on electromagnetic radiation from each wind turbine assumed in the example. Numerical values are identical to NB30, but the measurement distance is larger.

Further, we assume a receiver antenna gain of 10 dBi, a nacelle height of 70 m above terrain, and a ground conductivity of 3 mS/m.

The following messages are output to screen during initial geometrical evaluations:

```
Distance between receiver and wind farm centroid:    12.01 km
Distance between receiver and nearest wind turbine:  9.80 km
Distance between receiver and farthest wind turbine: 14.53 km

Average terrain elevation between wind farm and receiver: 21.6 m
Maximum terrain elevation of wind turbines:               30.0 m
Terrain elevation at receiver site:                       3.0 m
     Height above ground for GRWAVE: Wind farm generators at 78.4 m,
     receiver at 0.0 m

Lower frequency limit of GRWAVE for the given geometry is 61 kHz
```

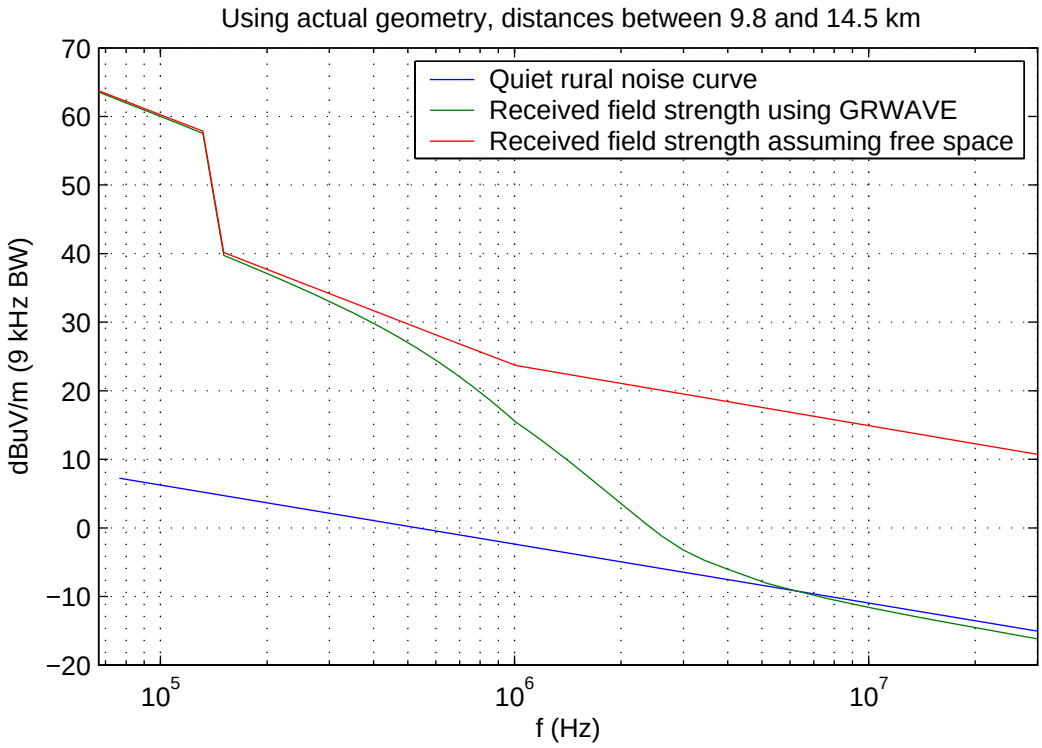

Figure 3.2 Electric field strength at the receiver site in the example, assuming the radiation from each wind turbine is at the limit level assumed.

The resulting EMI electric field strength predicted at the receiver site, resulting if all wind turbines radiate at the assumed limit level at all frequencies, is shown as the green curve in Fig. 3.2. We note that below 500 kHz, GRWAVE predictions are close to the free space equation and the interference is predicted to be more than 30 dB above the quiet rural curve. Above 4 MHz, the interference is predicted to be near or below the quiet rural noise curve, and will thus not increase the noise floor significantly.

If this was a real case, one would need to consider decreasing the limit level at the lower frequencies, relative to what was assumed in Fig. 3.1.

4 ELECTROMAGNETIC SCATTERING FROM WIND FARMS

4.1 Background

Modelling of EM scattering from wind farms at frequencies below 30 MHz is a sparse field in the open literature, and the work presented below is inspired by the Swedish report [11] and our experiences from the measurement campaign at Smøla [14].

In this chapter we propose a relatively simple model, designed to obtain order of magnitude estimates of the scattering effects from wind farms. The modest goal for the accuracy of the model is related to large uncertainties in several input parameters. We will refer to the prior Swedish model presented in [11] as “the FOI model” (FOI, Totalförsvarets Forskningsinstitut, is the Swedish equivalent to FFI), and stress the similarities and differences between the two models.

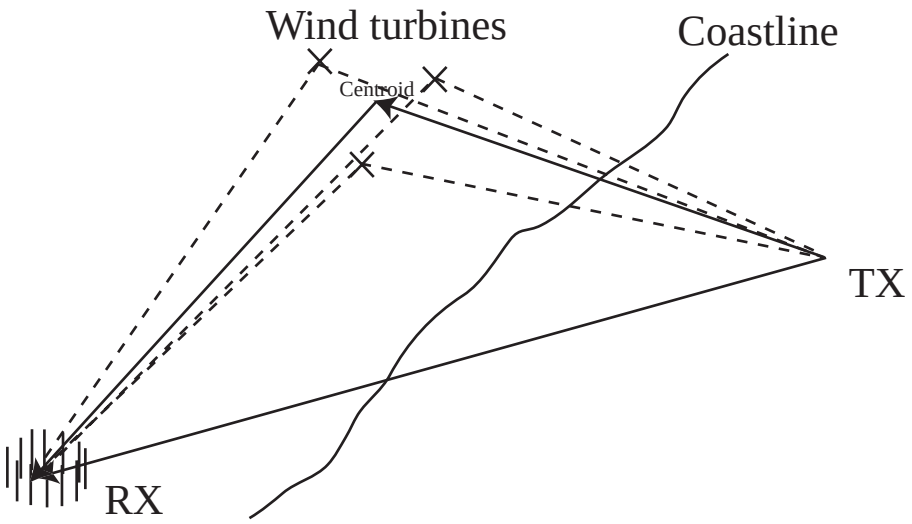

Figure 4.1 Wind farm scattering model, showing an on-shore wind farm containing three wind turbines.

We use Fig. 4.1 to illustrate the discussion. Note that this figure shows an on-shore wind farm, which is the case historically most common in Norway. In Sweden, off-shore wind farms has been a more prominent issue, and in that case the coastline should be drawn between the wind farm and the receiver.

4.1.1 Basic principle of models

Common to our model and the FOI model is that scattering from the entire wind farm is modelled by coherently summing the scattering effects from each wind turbine, as shown by

the dashed lines in Fig. 4.1. Multiple reflections and mutual coupling between wind turbines are ignored. The magnitude of the error introduced by this assumption is unknown, and numerical EM modelling of the entire wind farm would be required in order to quantify the effects. There is unfortunately not room for such modelling in the present FFI project. However, it is intuitively likely that ignoring mutual coupling is a severe source of error if the minimum distance between wind turbines is smaller than $\lambda/2$, where $\lambda = c/f$ is the wavelength.

4.1.2 Path loss

The FOI model applies the free space path loss for all paths. This is a good approximation over sea (i.e., for off-shore wind farms and coastal receiver sites), but introduces an error of tens of dB over land (see Figs. 2.2-2.3).

In our model, we estimate the ground wave path loss using GRWAVE for land paths, and use the Millington extension for paths crossing partly sea and partly land. This is more exact, but requires a specific modularization of the model (see Sec. 4.1.4 below).

4.1.3 Scattering from a single wind turbine

The FOI model includes pre-computed numerical EM models of scattering from a selection of simple wind turbines. These models are computed assuming the wind turbine is installed over a perfectly conducting ground, which is a good approximation for off-shore wind farms, but not true for on-shore wind farms. While the FOI model includes variation of scattering amplitude and phase with angle, distance, and frequency, we rather model the scattering amplitude and phase to be independent of angle, and hence given by a single RCS (radar cross section) value, at each frequency.

Fig. 4.2 is extracted from the numerical model of an 80 m high conical wind turbine with a 3-blade rotor of 40 m radius. This numerical model was supplied by FOI, and is identical to the one used in [11]. The figure shows the maximum variation with angle of RCS and scattering phase in the far field, as function of frequency. This indicates that assuming the RCS and scattering phase being independent of angle is a relatively good approximation at frequencies below approximately 10 MHz.

We note that the FOI model predicts the RCS of a single wind turbine to be 40-50 dBm^2 in the frequency range 2-20 MHz. However, according to [14], measurements at Smøla indicate an RCS per wind turbine of approximately 70 dBm^2 at 2.2 MHz and 85 dBm^2 at 10 MHz. This gives rise to large uncertainties regarding this important input parameter. Possible reasons for the discrepancy are

- The measurement data set from Smøla is very limited, and hence there are large uncertainties associated with the conclusions.
- The value 70 dBm^2 at 2.2 MHz corresponds to extreme phase fluctuations observed with the wind farm between transmitter and receiver (see [14, Sec. 4.13]). Uncertainty

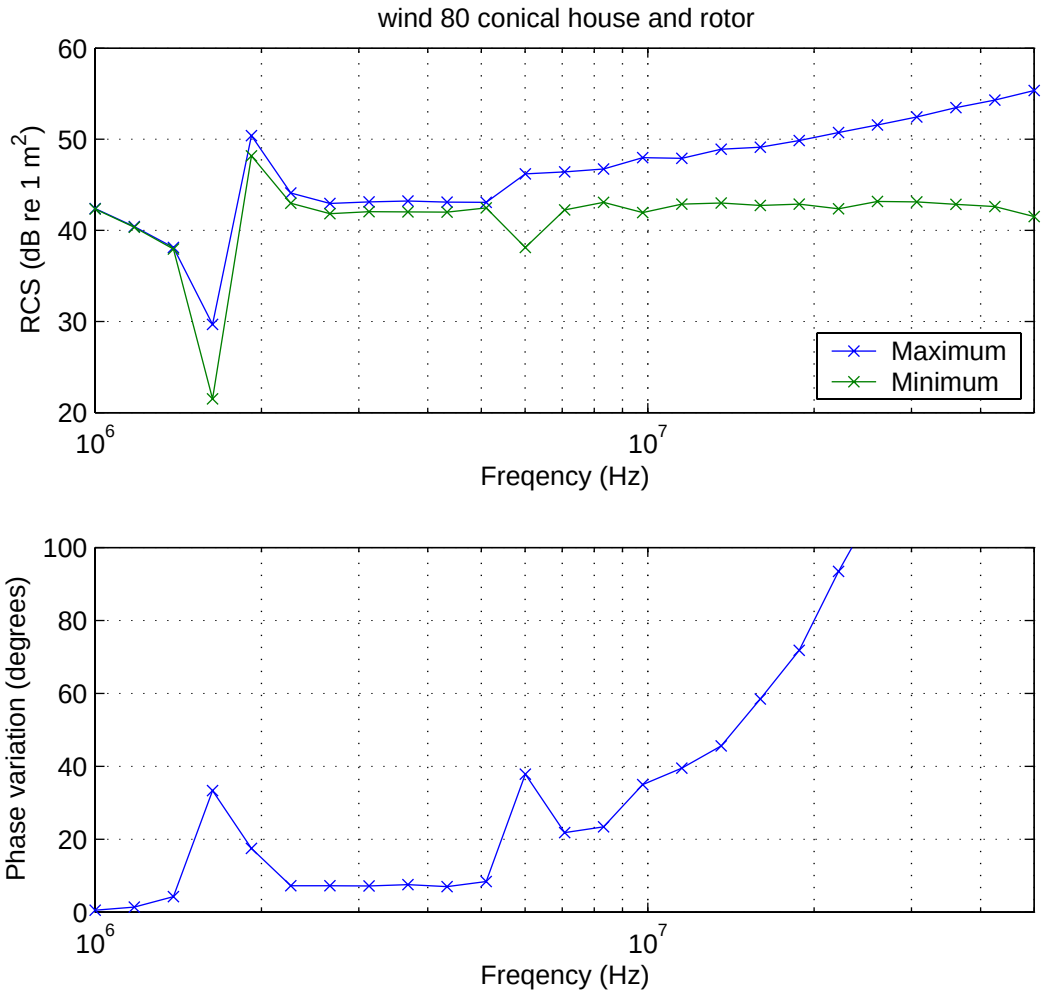

Figure 4.2 Numerical scattering model obtained from FOI of an 80 m high wind turbine, at infinite distance (far field). Upper plot: Maximum and minimum RCS over all angles. Lower plot: Variation in scattering phase over all angles.

remains as to whether the physical cause of this effect is related to scattering, shadowing, or both.

- The FOI model assumes the wind turbine to be mounted on a perfect ground plane, which is a good approximation at sea but not necessarily on land.

- The actual path loss at Smøla may for some reason be smaller than that predicted by GRWAVE at Smøla and used in [14]. Incidentally, if the free space equation is applied, the reduced path loss compared to GRWAVE will almost exactly cancel the discrepancy. We do, however, not see any physical reason to apply the free space equation for the path between wind farm and receiver at Smøla.

- Mutual coupling and multiple scattering between wind turbines may give rise to an "array factor" far above what is predicted by assuming coherent summation of independent scatterers. This can only be verified by generating a numerical EM model of the entire wind farm. Note, however, that the spacing between wind turbines is larger than one wavelength for both measurement frequencies.

We do not find it possible to conclude further on this issue based on the data currently available.

4.1.4 Modularization

The FOI model takes all the dashed lines in Fig. 4.1 into account throughout the computation, and considers the different arrival angles of each path when estimating the angular error of direction finding algorithms.

In our model, we use a two-step modularized approach as follows:

1. Estimate the "array factor" for the given wind farm and receiver geometry, for different transmitter positions. In this computation, the dashed lines of Fig. 4.1 are used. The array factor describes how much larger the RCS of the entire wind farm is, relative to the RCS of a single turbine.

2. The wind farm is replaced by a single scatterer positioned in the geographical centroid (average latitude and longitude) of the wind farm, with total RCS as determined in step 1 above. The bistatic radar equation is then applied using the solid lines of Fig. 4.1, with the free space equation replaced by GRWAVE predictions (with Millington extension if necessary).

Details on the operations in each step are outlined in the following paragraphs.

4.1.4.1 Step 1 – Array factor

The array factor χ_N of the entire wind farm is determined by the coherent summation equation (derived from [14, Eqn. (3.6)])

$$\chi_N(\text{RX pos}, \text{TX pos})[\text{dB}] = 20\log_{10}\left|\sum_{i=1}^{N} e^{jk(d_{RX,i}+d_{TX,i})}\left(\frac{\bar{d}_{RX}}{d_{RX,i}}\right)^{x}\left(\frac{\bar{d}_{TX}}{d_{TX,i}}\right)^{x}\right| \tag{4.1}$$

Here, $d_{RX,i}$ and $d_{TX,i}$ are the distances from the ith wind turbine to the receiver (transmitter), $\bar{d}_{RX}$ and $\bar{d}_{TX}$ distances from the wind farm centroid to the receiver (transmitter), $k = 2\pi/\lambda$ is the wave number, and x is the path loss amplitude exponent. x is found by investigating the GRWAVE slope between the minimum and maximum value of $d_{RX,i}$, and is defined such that 20 dB/decade (free space) corresponds to $x = 1$. Over land, we often have $x \approx 2$.

If the transmitter is far away, such that the signal can be modelled as a plane wave incident on the entire wind farm (e.g., by sky wave), Eqn. (4.1) becomes

$$\chi_N(\text{RX pos}, \text{TX pos})[\text{dB}] = 20\log_{10}\left|\sum_{i=1}^{N} e^{jk(d_{RX,i}+\mathbf{e}_I\cdot(\mathbf{r}_i-\bar{\mathbf{r}})}\left(\frac{\bar{d}_{RX}}{d_{RX,i}}\right)^{x}\right| \tag{4.2}$$

where $\mathbf{e}_I$ is a unit vector pointing in the direction of incidence (azimuth and possibly elevation) and $\mathbf{r}_i - \bar{\mathbf{r}}$ is the distance vector from the wind farm centroid to each wind turbine.

4.1.4.2 Step 2 – Bistatic radar equation

The path loss L for each of the three solid lines in Fig. 4.1 is estimated using GRWAVE, with the Millington extension if necessary. Then, the ratio K_s between the scattered and the direct signal is computed as follows (derived from [14, Eqn. (3.5)])

$$\begin{aligned} K_s[\text{dB}] = &-158.55 + 20\log_{10}(f[\text{Hz}]) + \sigma_1[\text{dBm}^2] + \chi_N[\text{dB}] \\ &- L_{\text{Windfarm-RX}}[\text{dB}] - L_{\text{TX-Windfarm}}[\text{dB}] + L_{\text{TX-RX}}[\text{dB}] \end{aligned} \tag{4.3}$$

Here, σ_1 is the RCS of a single wind turbine, χ_N is the array factor, and the last three terms represent the difference between path loss of the direct path and total path losses of the scattered paths.

If the transmitter is far away (e.g., by sky wave), the last two loss terms are approximately identical and Eqn. (4.3) becomes

$$K_s[\text{dB}] = -158.55 + 20\log_{10}(f[\text{Hz}]) + \sigma_1[\text{dBm}^2] + \chi_N[\text{dB}] - L_{\text{Windfarm-RX}}[\text{dB}] \tag{4.4}$$

4.1.5 Direction finding error

In the FOI model, the angular error is estimated directly, referring to certain specific direction finding algorithms.

Our model is designed to be independent of knowledge on direction finding algorithms, and hence the output is given as the ratio K_s between scattered and direct signal rather than as angular error. Also, information on angular spread of the scattered paths are lost in the modularization applied, complicating exact computations of direction finding error.

To give an idea of the meaning of numerical values of K_s, we have estimated the direction finding error for a simple two-antenna interferometer. Assuming that the direct signal is incident on the interferometer from the broadside direction, the ratio between the signals (complex baseband equivalent) at the two antennas is

$$\frac{V_2}{V_1} = \frac{1 + k_s e^{jka\sin(\alpha_r)+\theta}}{1 + k_s e^{j\theta}} \tag{4.5}$$

where $k_s = 10^{K_s/20}$ is the amplitude ratio corresponding to K_s in dB units, α_r is the angle of incidence of the scattered path relative to the broadside direction, θ is the (arbitrary) phase difference between the two paths, k is the wave number, and a is the separation between the two receiver antennas. By geometrical considerations we find that the worst-case angular error results when $ka\sin(\alpha_r) = \pm\pi/2$, and θ is equal to 0 or π. In this case, Eqn. (4.5) simplifies to

$$\left(\frac{V_2}{V_1}\right)_{\text{Worst case}} = \frac{1 \pm jk_s}{1 \pm k_s} \tag{4.6}$$

The interferometer only considers the phase of V_2/V_1, hence the real-valued denominator is irrelevant. While the phase should ideally be zero, corresponding to the broadside direct path, the phase resulting from the combination of direct and scattered path is

$$\phi_{e,\text{Worst case}} = \angle\left(\frac{V_2}{V_1}\right)_{\text{Worst case}} = \tan^{-1} k_s \tag{4.7}$$

Further, the relationship between phase ϕ and arrival angle α for a simple interferometer is $\phi = ka\sin(\alpha)$, hence the worst case angular error becomes

$$\alpha_{e,\text{Worst case}} = \sin^{-1}\frac{\tan^{-1} k_s}{ka} \tag{4.8}$$

When $a = \lambda/2$ (half-wavelength antenna separation), we have $ka = \pi$. In this case, the worst case corresponds to the scattered path entering at an angle of $\alpha_r = 30^\circ$ relative to broad-side. Fig. 4.3 shows the worst case error as function of K_s, for the case of $a = \lambda/2$. In particular, we note that $K_s = -25$ dB corresponds to $\alpha_e \leq 1^\circ$, while $K_s = -5$ dB corresponds to $\alpha_e \leq 10^\circ$.

Note that the derivation of worst case angular errors above is only valid for $a \geq \lambda/4$, as it is not possible to reach the worst-case condition of $ka\sin(\alpha_r) = \pm\pi/2$ for smaller antenna separations. For smaller antenna separations, the worst case is $\sin(\alpha_r) = \pm 1$ and $\theta = \pi$, in which case we obtain (derivation details are skipped, but are similar to the derivation for larger antenna separations above)

$$\alpha_{e,\text{Worst case, small } a} = \sin^{-1}\frac{\tan^{-1}\frac{k_s\sin(ka)}{1-k_s\cos(ka)}}{ka} \tag{4.9}$$

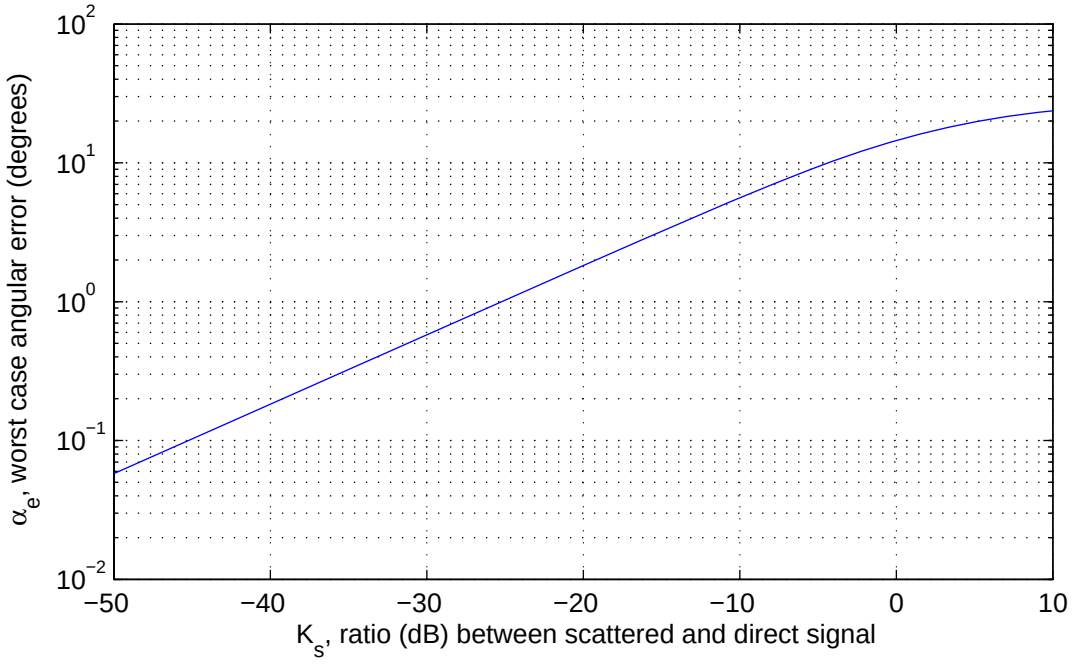

Figure 4.3 *Worst-case direction finding error as function of K_s for a simple interferometer, with half-wavelength antenna separation and the direct path incident at broadside.*

4.2 Recommendations

In this section we present recommendations on usage and parameter settings, when applying the scattering model developed in the present work.

4.2.1 Frequency range

The lower frequency limit at which multiple scattering and mutual reflections can be ignored is not exactly known to us, but using the model when separations between wind turbines is smaller than $\lambda/2$ is not recommended (see Sec. 4.1.1). Thus, we do not recommend applying the model at frequencies below

$$f_{\text{min}} = \frac{c}{2\delta} \tag{4.10}$$

where c is the speed of light and δ is the smallest separation between any pair of wind turbines in the wind farm.

As seen in Fig. 4.2, assuming the RCS and scattering phase of a single wind turbine to be independent of angle may introduce severe errors at frequencies larger than 10 MHz. Thus, we do not recommend applying the model at frequencies above

$$f_{\text{max}} = 10 \text{ MHz} \tag{4.11}$$

4.2.2 RCS value of a single wind turbine

As discussed in Sec. 4.1.3, there are large discrepancies between the RCS value resulting from FOI's numerical model of a single wind turbine, and the RCS value per wind turbine deduced from the measurement campaign at Smøla. Due to the limited data set from Smøla, there are however large uncertainties associated with this value, and further measurements would be required in order to make firmer estimates.

Based on the data currently available, the RCS value σ_1 of a single wind turbine can be anywhere between 45 and 85 dBm^2, in the frequency range 2-10 MHz. For the time being, we recommend using the value

$$\sigma_1 = 65 \text{ dBm}^2 \tag{4.12}$$

We do not see any reason to include frequency-dependency in σ_1 at this stage, as the uncertainties are large anyway.

If further measurements are performed in the future, this value (and possible frequency-dependency) should be updated based on the new information.

4.2.3 Interpretation of output

The output from our model is the ratio K_s between scattered and direct signal, given in dB. We recommend that the relationship between K_s and direction finding error is investigated for the particular equipment and algorithms used at the receiver location, and a threshold for K_s is set on this basis.

If it is not possible or desirable to establish such a relationship for the specific algorithms used, we recommend setting thresholds based on the worst-case expressions for a simple interferometer in Sec. 4.1.5. Referring to the antenna separation as a, we then make the following recommendations:

- For $a < \lambda/4$, Eqn. (4.9) should be used.
- For $a \geq \lambda/4$, Eqn. (4.8) should be used.
- For $a = \lambda/2$, this relationship is shown in Fig. 4.3, where we note that $K_s = -25$ dB corresponds to a maximum DF error of 1°.

4.3 Implementation

The model described above has been implemented as a Matlab function *windfarm_HF_scattering.m*, which takes the following input parameters:

- Geographical coordinates of wind farm and receiver
- Frequency(ies) for evaluation

- Ground conductivity (permittivity is derived from conductivity as described in Sec. 2.2)
- RCS per wind turbine (constant, or function of frequency)
- Switch specifying whether to evaluate far-away transmitters, nearby transmitters, or both
- Geometrical parameters (azimuth angular resolution and incident elevation angle for far-away transmitters; geographical area and grid resolution for nearby transmitters)
- Flag specifying whether plots should be produced or not

The output of the function is the resulting ratio K_s between the scattered and direct path, as function of azimuth angle (far-away transmitters) or geographical position (nearby transmitters). For nearby transmitters, the result may be plotted in a map.

For the time being, the implementation only supports the case where wind farm and receiver is on land (but the transmitter may be at sea). For study of off-shore wind farms, the software requires extensions which should be relatively straightforward.

The function uses digital elevation data on the DTED format to evaluate the terrain profile along the path between wind farm centroid and receiver, from which the average elevation of the path is computed. Then, the transmitter and receiver heights *for the path between wind farm and receiver* are set according to the recommendations in Sec. 2.2, assuming all turbines are at the same terrain elevation as the highest wind turbine. *For the paths from transmitter to wind farm and receiver*, all antenna heights are for simplicity set equal to zero.

The path loss amplitude exponent x vs distance in Eqns. (4.1)-(4.2) is determined from GRWAVE path loss predictions at two points, which are the distances from the receiver to the nearest and farthest wind turbine.

The path loss from the transmitter to the wind farm and to the receiver is approximated as follows: When evaluating nearby transmitter positions, the DTED map is used to determine whether the transmitter is at sea or on land. If the transmitter is on land, GRWAVE is applied assuming there is land along the entire path from transmitter to wind farm/receiver. If the transmitter is at sea, Millington's method is applied assuming there is one single sea/land-transition, whose location is determined by the relative amount of sea and land along the path from transmitter to wind farm/receiver.

In order to increase efficiency, the model uses precomputed tables of Millington path loss for different parameter combinations (ground type, frequency, path length, transition distance), applying a combination of table lookup and interpolation during run-time.

This model is planned for integration into WTES.

4.4 Example

As an example, we revisit the geometry from the measurement campaign at Smøla [14], shown in Fig. 4.4. The RCS per wind turbine is assumed to be 65 dBm^2 at all frequencies, and the

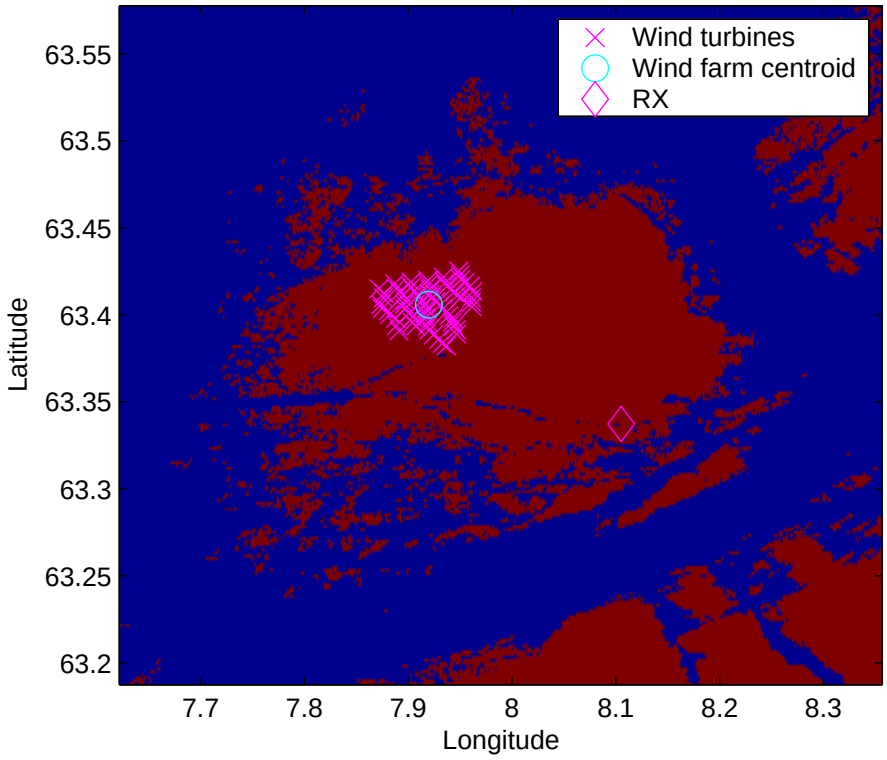

Figure 4.4 Map showing wind turbine and receiver locations for the example using the geometry from the measurement campaign at Smøla.

ground conductivity is 3 mS/m. For far-away transmitters, the incident elevation angle is set equal to 0.

The following messages are output to screen while running the model:

```
Minimum separation between turbines: 228 m
Lowest recommended frequency for model: 0.66 MHz

Distance between receiver and wind farm centroid:    12.01 km
Distance between receiver and nearest wind turbine:  9.80 km
Distance between receiver and farthest wind turbine: 14.53 km

Average terrain elevation between wind farm and receiver: 21.6 m
Maximum terrain elevation of wind turbines:               30.0 m
Terrain elevation at receiver site:                       3.0 m
     Height above ground for GRWAVE: Wind farm at 8.4 m,
     receiver at 0.0 m

Please wait while evaluating path losses
     from all transmitter positions to wind farm
Please wait while evaluating path losses
     from all transmitter positions to receiver
Done!
```

For far-away transmitters, the result is visualized in two different ways in Figs. 4.5-4.6. At all

frequencies, the maximum predicted scattering amplitude in Fig. 4.6 occurs when the transmitter is behind the wind farm as seen from the receiver (about -50° in Fig. 4.5).

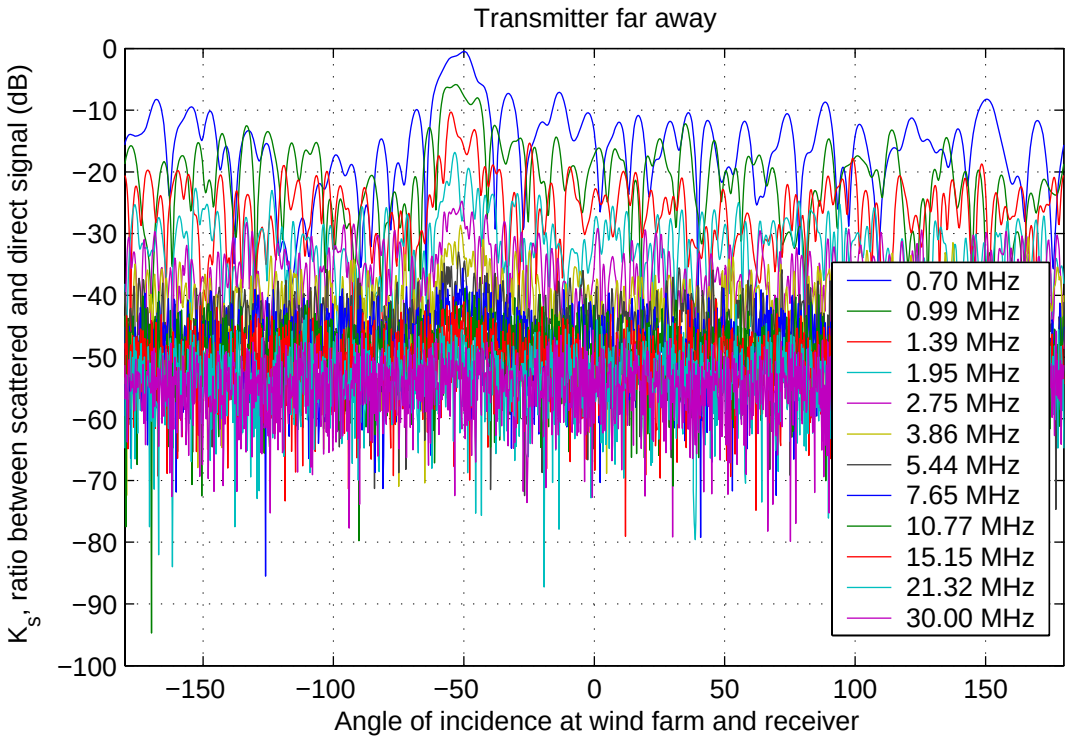

Figure 4.5 Example result for far-away transmitter, as function of azimuth angle of incidence (0=North, 90=East).

For nearby transmitters, the result is visualized in a map as shown in Fig. 4.7 (one such map is produced per evaluation frequency), and as function of frequency as shown in Fig. 4.8. The latter plot shows the maximum scattering over all *sea* squares; in practice this is the result when the transmitter is located in the sea square closest to the wind farm. Note that the maximum scattering amplitudes are also for nearby transmitters predicted to occur when the wind farm is between transmitter and receiver.

Note that in both cases (far-away and nearby transmitters), the model predicts the scattering to increase with decreasing frequency all the way down to the estimated lower frequency of validity for the model, which for the Smøla wind farm is 0.66 MHz. There is however great uncertainty associated with this prediction, as it is not known whether the RCS per turbine can still be assumed constant as the frequency decreases.

The results at 1.9 MHz (Fig. 4.7) are seen to be in approximate agreement with the measurement results at 2.2 MHz during the campaign at Smøla. This is not surprising, since the RCS value used in the example was originally extrapolated from the measurement campaign. The agreement seen between model and measurement can therefore honestly *NOT* be used as validation of the model, and the model can not be firmly validated without further measurement results.

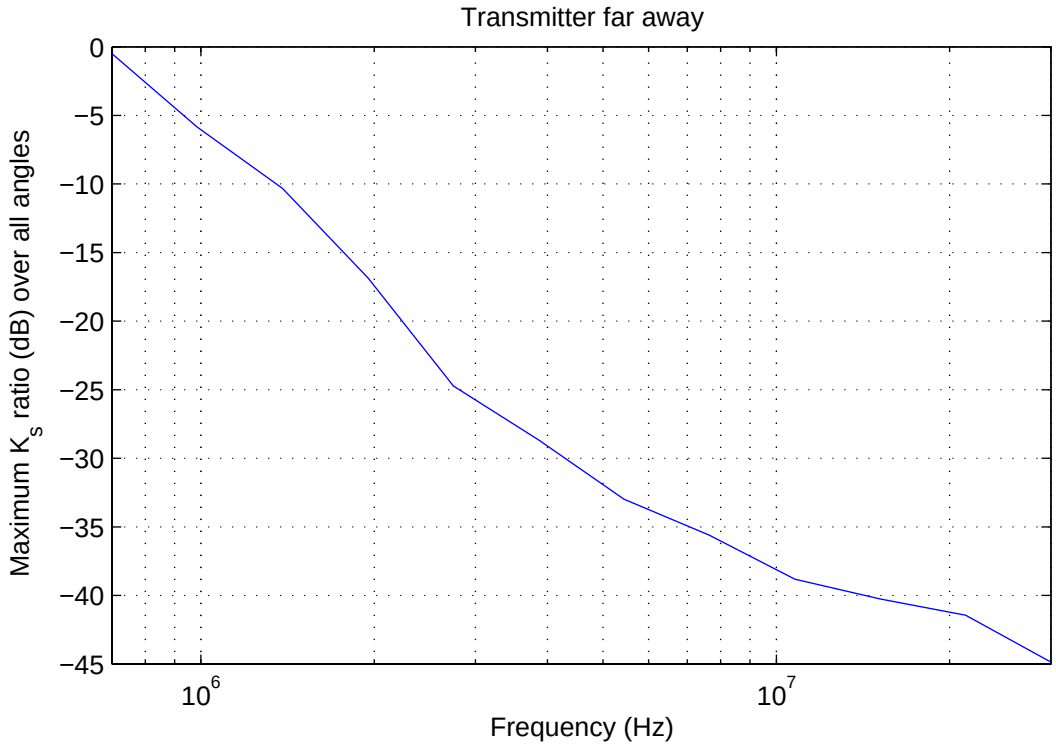

Figure 4.6 Example result for far-away transmitter, as function of frequency (maximum scattering over all azimuth angles of incidence).

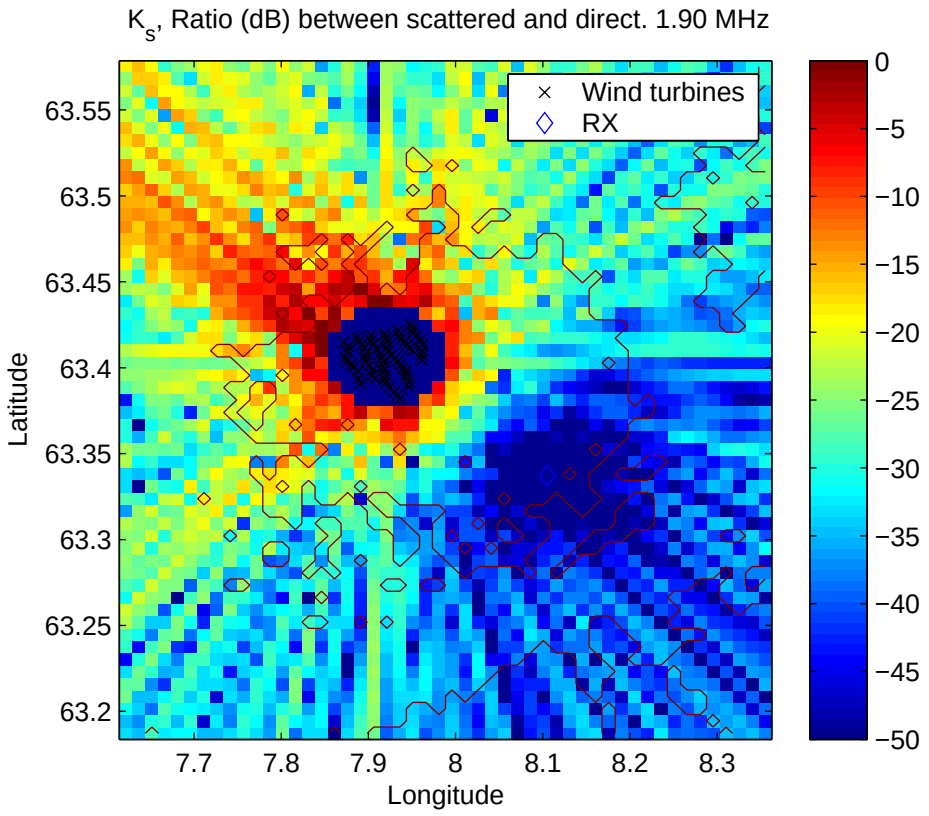

Figure 4.7 Example result for nearby transmitter at 1.9 MHz, shown in map.

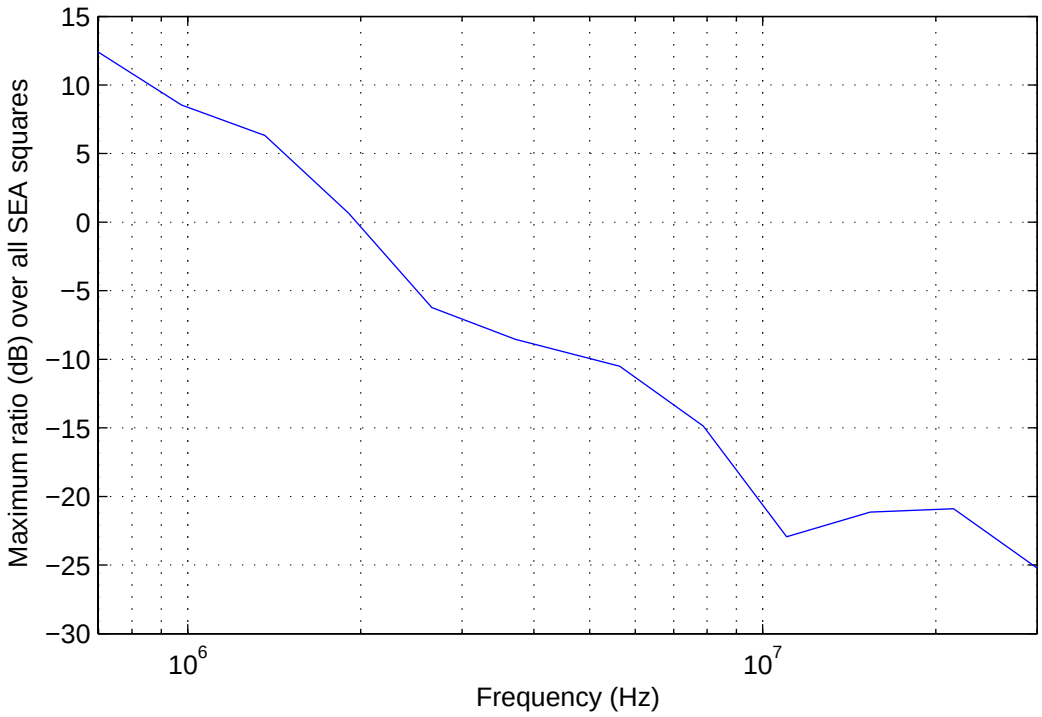

Figure 4.8 Example result for nearby transmitter as function of frequency (maximum scattering over all sea *squares)*

5 CONCLUSIONS

Mathematical prediction models for electromagnetic influences from wind farms (radiation and scattering), at frequencies below 30 MHz, have been presented. The models are presently implemented as Matlab functions. Recommendations on usage and parameter settings are included in the report. Examples have been presented using the geometry from the measurement campaign at Smøla.

The model for electromagnetic interference due to radiation from the wind turbines basically extrapolates the electrical field strength from the distance at which the measurement is performed to the distance between the wind farm and the receiver. The extrapolation is based on well established propagation models. Additionally, the receiver antenna gain and the cumulative effect due to the number of wind turbines is taken into account.

The remaining challenge regarding radiation is to agree on field strength limits, measurement distance, and measurement methodology. Ideally, *in situ* compliance measurements should be performed with the measurement antenna in the same horizontal plane as the generator, which calls for a long non-conductive mast or a wire from a helicopter.

The design goal for the electromagnetic scattering model was to provide order-of-magnitude estimates on the ratio between scattered and direct signal strength. The model is based on coherent summation of scattering from the individual wind turbines. The model suffers large uncertainties, in particular regarding the radar cross section per wind turbine (where there are large discrepancies between a numerical study by FOI and the measurement results from

Smøla), and the lower frequency limit at which the model is valid (before multiple reflections and mutual coupling between turbines must be taken into account). Further measurements would be required in order to validate and calibrate the model. It is the author's opinion that the scattering model presented in this report is the best obtainable based on the knowledge currently available to FFI.

6 ACKNOWLEDGMENTS

Tomas Boman at FOI in Sweden supplied information on their scattering model and the background material for Fig. 4.2. Stein Sørum at the EMC lab of the Norwegian Defence Logistic Organization (FLO) at Kjeller supplied background information and was a useful discussion partner regarding EMI.

Thanks are extended to both for their valuable contributions.

References

(1) (1992): Rec. ITU-R P.527-3: Electrical Characteristics of the Surface of the Earth.

(2) (1999): MIL-STD-461E: Requirements Fot the Control of Electromagnetic Interference Characteristics of Subsystems and Equipment. US Department of Defense, USA.

(3) (1999): Rec. ITU-R P-832-2: World Atlas of Ground Conductivites.

(4) (2001): Reg TP 322 MV 05 Part 1: Specification for the Measurement of Disturbance Fields from Telecommunications Systems and Networks in the Range 3 kHz to 3 GHz. For Application in Accordance with Paragraph (1) of Usage Provision No. 30 (NB 30) as in the Frequenzy Band Allocation Ordinance (FreqBZPV) Part B: Usage Provisions. Regulatory Authority for Telecommunications and Posts.

(5) (2003): CISPR 16-4-4: Specification for Radio Disturbance and Immunity Measuring Apparatus and Methods - Part 4-4: Uncertainties, Statistics and Limit Modelling - Statistics of Complaints and a Model for the Calculation of Limits.

(6) (2003): Rec. ITU-R P.372-8: Radio Noise.

(7) (2004): EN 55011 / CISPR 11: Industrial, Scientific and Medical (ISM) Radio-Frequency Equipment - Electromagnetic Disturbance Characteristics - Limits and Methods of Measurement. Edition 4.1.

(8) (2004): EN 55016-1-1 / CISPR 16-1-1: Specification for Radio Disturbance and Immunity Measuring Apparatus and Methods - Part 1-1: Radio Disturbance and Immunity Measuring Apparatus - Measuring Apparatus. Incorporating Amendment No. 1.

(9) (2004): EN 55016-1-4 / CISPR 16-1-4: Specification for Radio Disturbance and Immunity Measuring Apparatus and Methods - Part 1-4: Radio Disturbance and Immunity Measuring Apparatus - Ancillary Equipment - Radiated Disturbances.

(10) (2004): EN 55016-2-3 / CISPR 16-2-3: Specification for Radio Disturbance and Immunity Measuring Apparatus and Methods - Part 2-3: Methods of Measurement of Disturbances and Immunity - Radiated Disturbance Measurements.

(11) Boman T and Petterson L (2000): Direction Finding Error Due to Scattering from Wind Mills, Analysis and Computations. Scientific report FOA-R–00-01522-616–SE, FOI, Linköping, Sweden.

(12) Hvidsten K I (2005): A Comparison Between Measurements and Predictions of HF Groundwave Propagation. FFI/RAPPORT 2005/01703, FFI, Kjeller, Norway.

(13) (1992): Rec. ITU-R P.368-7: Ground-Wave Propagation Curves for Frequencies Between 10 kHz and 30 MHz.

(14) Otnes R and Hjelmstad J (2006): Observability at HF Direction Finding Sites of Scattering from Wind Farms - Measurements at Smøla 2006. FFI/RAPPORT 2006/02701.

APPENDIX

A ACRONYMS

CISPR	Comite International Special des Perturbations Radioelectrique
DF	Direction Finding
DTED	Digital Terrain Elevation Data
EM	Electromagnetic
EMC	Electromagnetic compatibility
EMI	Electromagnetic interference
EN	Europäische Norm
FOI	Totalförsvarets Forskningsinstitut (Sweden)
HF	High Frequency (2-30 MHz)
ITU-R	International Telecommunication Union – Radiocommunication
MIL-STD	Military Standard (USA)
NB	Nutzungsbestimmung
RCS	Radar cross section
WTES	Wind Turbines & Electromagnetic Systems